Research Article | Vol. 26, No. 8 | 16 Apr 2018 | OPTICS EXPRESS 9963
Optics EXPRESS

Efficient half-harmonic generation of three-optical-cycle mid-IR frequency comb around 4 μm using OP-GaP

EVGENI SOROKIN,[1] ALIREZA MARANDI,[2,*] PETER G. SCHUNEMANN,[3] M. M. FEJER,[2] ROBERT L. BYER,[2] AND IRINA T. SOROKINA[4]

[1]*Photonics Institute, Vienna University of Technology, 1040 Vienna, Austria*
[2]*E. L. Ginzton Laboratory, Stanford University, Stanford, CA 94305, USA*
[3]*BAE Systems, P. O. Box 868, MER15-1813, Nashua, New Hampshire 03061-0868, USA*
[4]*Department of Physics, Norwegian University of Science and Technology, N-7491 Trondheim, Norway*
**marandi@stanford.edu*

Abstract: We report a broadband mid-infrared frequency comb with three-optical-cycle pulse duration centered around 4.2 μm, via half-harmonic generation using orientation-patterned GaP (OP-GaP) with ~43% conversion efficiency. We experimentally compare performance of GaP with GaAs and lithium niobate as the nonlinear element, and show how properties of GaP at this wavelength lead to generation of the shortest pulses and the highest conversion efficiency. These results shed new light on half-harmonic generation of frequency combs, and pave the way for generation of short-pulse intrinsically-locked frequency combs at longer wavelengths in the mid-infrared with high conversion efficiencies.

OCIS codes: (190.4970) Parametric oscillators and amplifiers; (190.7110) Ultrafast nonlinear optics; (140.3510) Lasers, fiber; (140.3070) Infrared and far-infrared lasers.

References and links

1. I. Coddington, W. C. Swann, and N. R. Newbury, "Coherent Multiheterodyne Spectroscopy Using Stabilized Optical Frequency Combs," Phys. Rev. Lett. **100**(1), 013902 (2008).
2. G. B. Rieker, F. R. Giorgetta, W. C. Swann, J. Kofler, A. M. Zolot, L. C. Sinclair, E. Baumann, C. Cromer, G. Petron, C. Sweeney, P. P. Tans, I. Coddington, and N. R. Newbury, "Frequency-comb-based remote sensing of greenhouse gases over kilometer air paths," Optica **1**(5), 290–298 (2014).
3. B. Bernhardt, E. Sorokin, P. Jacquet, R. Thon, T. Becker, I. T. Sorokina, N. Picqué, and T. W. Hänsch, "Mid-infrared dual-comb spectroscopy with 2.4 μm Cr2+:ZnSe femtosecond lasers," Appl. Phys. B **100**(1), 3–8 (2010).
4. F. Keilmann, C. Gohle, and R. Holzwarth, "Time-domain mid-infrared frequency-comb spectrometer," Opt. Lett. **29**(13), 1542–1544 (2004).
5. K. A. Tillman, R. R. J. Maier, D. T. Reid, and E. D. McNaghten, "Mid-infrared absorption spectroscopy of methane using a broadband femtosecond optical parametric oscillator based on aperiodically poled lithium niobate," J. Opt. A, Pure Appl. Opt. **7**(6), S408–S414 (2005).
6. M. W. Haakestad, T. P. Lamour, N. Leindecker, A. Marandi, and K. L. Vodopyanov, "Intracavity trace molecular detection with a broadband mid-IR frequency comb source," J. Opt. Soc. Am. B **30**(3), 631–640 (2013).
7. E. Sorokin, I. T. Sorokina, J. Mandon, G. Guelachvili, and N. Picque, "Sensitive multiplex spectroscopy in the molecular fingerprint 2.4 μm region with a Cr2+:ZnSe femtosecond laser," Opt. Express **15**(25), 16540–16545 (2007).
8. C. Y. Wang, T. Herr, P. Del'Haye, A. Schliesser, J. Hofer, R. Holzwarth, T. W. Hänsch, N. Picqué, and T. J. Kippenberg, "Mid-infrared optical frequency combs at 2.5 μm based on crystalline microresonators," Nat. Commun. **4**, 1345 (2013).
9. S. T. Wong, K. L. Vodopyanov, and R. L. Byer, "Self-phase-locked divide-by-2 optical parametric oscillator as a broadband frequency comb source," J. Opt. Soc. Am. B **27**(5), 876–882 (2010).
10. A. Marandi, N. C. Leindecker, V. Pervak, R. L. Byer, and K. L. Vodopyanov, "Coherence properties of a broadband femtosecond mid-IR optical parametric oscillator operating at degeneracy," Opt. Express **20**(7), 7255–7262 (2012).
11. A. Marandi, K. A. Ingold, M. Jankowski, and R. L. Byer, "Cascaded half-harmonic generation of femtosecond frequency combs in the mid-infrared," Optica **3**(3), 324–327 (2016).

#323172 https://doi.org/10.1364/OE.26.009963
Journal © 2018 Received 13 Feb 2018; revised 1 Apr 2018; accepted 2 Apr 2018; published 6 Apr 2018

Optics EXPRESS

12. S. T. Wong, T. Plettner, K. L. Vodopyanov, K. Urbanek, M. Digonnet, and R. L. Byer, "Self-phase-locked degenerate femtosecond optical parametric oscillator," Opt. Lett. **33**(16), 1896–1898 (2008).
13. N. Leindecker, A. Marandi, R. L. Byer, and K. L. Vodopyanov, "Broadband degenerate OPO for mid-infrared frequency comb generation," Opt. Express **19**(7), 6296–6302 (2011).
14. C. W. Rudy, A. Marandi, K. A. Ingold, S. J. Wolf, K. L. Vodopyanov, R. L. Byer, L. Yang, P. Wan, and J. Liu, "Sub-50 fs pulses around 2070 nm from a synchronously-pumped, degenerate OPO," Opt. Express **20**(25), 27589–27595 (2012).
15. N. Leindecker, A. Marandi, R. L. Byer, K. L. Vodopyanov, J. Jiang, I. Hartl, M. Fermann, and P. G. Schunemann, "Octave-spanning ultrafast OPO with 2.6-6.1 μm instantaneous bandwidth pumped by femtosecond Tm-fiber laser," Opt. Express **20**(7), 7046–7053 (2012).
16. K. L. Vodopyanov, E. Sorokin, I. T. Sorokina, and P. G. Schunemann, "Mid-IR frequency comb source spanning 4.4-5.4 μm based on subharmonic GaAs optical parametric oscillator," Opt. Lett. **36**(12), 2275–2277 (2011).
17. V. O. Smolski, S. Vasilyev, P. G. Schunemann, S. B. Mirov, and K. L. Vodopyanov, "Cr:ZnS laser-pumped subharmonic GaAs optical parametric oscillator with the spectrum spanning 3.6-5.6 μm," Opt. Lett. **40**(12), 2906–2908 (2015).
18. V. Smolski, S. Vasilyev, I. Moskalev, M. Mirov, A. Muraviev, S. Mirov, K. Vodopyanov, and V. Gapontsev, "Sub-Watt Femtosecond Laser Source with the Spectrum Spanning 3-8 μm," in Laser Congress 2017 (ASSL, LAC), OSA Technical Digest (online) (Optical Society of America, 2017), AM4A.6.
19. V. Tassev, M. Snure, R. Petterson, K. L. Schepler, R. G. Bedford, J. M. Mann, S. Vangala, W. Goodhue, A. Lin, J. S. Harris, M. Fejer, P. G. Schunemann, "Recent Progress in Development Orientation-Patterned GaP for Next-Generation Frequency Conversion Devices," in *CLEO: 2013*, OSA Technical Digest (online) (Optical Society of America, 2013), paper JM4K.5.
20. P. G. Schunemann, K. T. Zawilski, L. A. Pomeranz, D. J. Creeden, and P. A. Budni, "Advances in nonlinear optical crystals for mid-infrared coherent sources," J. Opt. Soc. Am. B **33**(11), D36–D43 (2016).
21. Q. Ru, Z. E. Loparo, X. Zhang, S. Crystal, S. Vasu, P. G. Schunemann, and K. L. Vodopyanov, "Self-referenced octave-wide subharmonic GaP optical parametric oscillator centered at 3 μm and pumped by an Er-fiber laser," Opt. Lett. **42**(22), 4756–4759 (2017).
22. L. Maidment, P. G. Schunemann, and D. T. Reid, "Molecular fingerprint-region spectroscopy from 5 to 12 μm using an orientation-patterned gallium phosphide optical parametric oscillator," Opt. Lett. **41**(18), 4261–4264 (2016).
23. E. Sorokin, A. Marandi, P. G. Schunemann, M. Fejer, I. T. Sorokina, R. L. Byer, "Three-optical-cycle frequency comb centered around 4.2 μm using OP-GaP-based half-harmonic generation," in *High Brightness Sources and Light-Driven Interactions*, OSA Technical Digest (Optical Society of America, 2016), paper MS3C.2.
24. T. Skauli, K. L. Vodopyanov, T. J. Pinguet, A. Schober, O. Levi, L. A. Eyres, M. M. Fejer, J. S. Harris, B. Gerard, L. Becouarn, E. Lallier, and G. Arisholm, "Measurement of the nonlinear coefficient of orientation-patterned GaAs and demonstration of highly efficient second-harmonic generation," Opt. Lett. **27**(8), 628–630 (2002).
25. I. Shoji, T. Kondo, A. Kitamoto, M. Shirane, and R. Ito, "Absolute scale of second-order nonlinear-optical coefficients," J. Opt. Soc. Am. B **14**(9), 2268–2294 (1997).
26. G. Insero, C. Clivati, D. D'Ambrosio, P. Natale, G. Santambrogio, P. G. Schunemann, J.-J. Zondy, and S. Borri, "Difference frequency generation in the mid-infrared with orientation-patterned gallium phosphide crystals," Opt. Lett. **41**(21), 5114–5117 (2016).
27. R. C. Miller, "Optical Second Harmonic Generation In Piezoelectric Crystals," Appl. Phys. Lett. **5**(1), 17–19 (1964).
28. R. L. Byer, "Nonlinear Optical Phenomena and Materials," Annu. Rev. Mater. Sci. **4**(1), 147–190 (1974).
29. M. Jankowski, A. Marandi, C. R. Phillips, R. Hamerly, K. A. Ingold, R. L. Byer, and M. M. Fejer, "Temporal Simultons in Optical Parametric Oscillators," Phys. Rev. Lett. **120**(5), 053904 (2018).
30. K. F. Lee, C. Mohr, J. Jiang, P. G. Schunemann, K. L. Vodopyanov, and M. E. Fermann, "Midinfrared frequency comb from self-stable degenerate GaAs optical parametric oscillator," Opt. Express **23**(20), 26596–26603 (2015).
31. O. H. Heckl, B. J. Bjork, G. Winkler, P. Bryan Changala, B. Spaun, G. Porat, T. Q. Bui, K. F. Lee, J. Jiang, M. E. Fermann, P. G. Schunemann, and J. Ye, "Three-photon absorption in optical parametric oscillators based on OP-GaAs," Opt. Lett. **41**(22), 5405–5408 (2016).
32. I. T. Sorokina, V. V. Dvoyrin, N. Tolstik, and E. Sorokin, "Mid-IR ultrashort pulsed fiber-based lasers," IEEE J. Sel. Top. Quantum Electron. **20**(5), 0903412 (2014).

1. Introduction

Broadband mid-infrared frequency combs are becoming increasingly important for applications such as trace gas sensing and stand-off molecular detection with high resolution, sensitivity, and fast acquisition rates [1–3]. Some of the techniques to produce mid-infrared frequency combs includes difference frequency generation [4], synchronously-pumped optical parametrical oscillators (OPO) [5, 6], mid-IR femtosecond lasers [7], and microresonators [8]. Of these techniques, half-harmonic generation, i.e. the inverse of second-

Optics EXPRESS

harmonic generation, using quasi-phase matched nonlinear media offers an unprecedented level of coherence transfer and efficiency [9–11]. The broadband infrared frequency combs in synchronously-pumped half-harmonic OPOs have been demonstrated using different combinations of nonlinear crystals and pump sources: periodically poled lithium niobate $LiNbO_3$ (PPLN) with Ti:sapphire [12], Er:fiber [13], and Yb:fiber [11, 14] femtosecond pump lasers, and orientation-patterned GaAs (OP-GaAs) with Tm-fiber [15], Cr:ZnSe [16], and Cr:ZnS [17, 18] femtosecond pump lasers. Lately, broadband intrinsically phase- and frequency-locked frequency combs with 50-fs pulses at 2 μm and 110-fs pulses at 4 μm have been produced via a two-stage cascaded half-harmonic generation in PPLN [11]. However, in previous demonstrations of half-harmonic generation in the mid-IR, achieving high conversion efficiencies and few-cycle pulses simultaneously has been challenging due to the linear and nonlinear properties of available materials.

Recently, a new quasi-phase-matched semiconductor, i.e. orientation-patterned gallium phosphide (OP-GaP), has become available using the all-epitaxial processing technique combined with optimized hydride vapor phase epitaxy to achieve parallel grating propagation to over 500 μm thicknesses [19]. Gallium phosphide has excellent characteristics for mid-IR parametric frequency conversion including the high nonlinear coefficient and wide transparency range. Compared to GaAs, it has lower nonlinear coefficient, but larger indirect band gap (Eg = 2.26 eV), which allows pumping at shorter wavelengths, and also lower group velocity dispersion (GVD) at $\lambda < \sim 5.5$ μm, simplifying the need for dispersion compensation. Lower dispersion also results in larger grating periods which can propagate more easily to large thicknesses providing large clear apertures. OP-GaP has been recently used in different types of wavelength conversion processes in the mid-IR including OPOs [20–23].

Following our preliminary demonstration of OP-GaP-based half-harmonic generation [23], here we report highly-stable efficient half-harmonic generation of a three-cycle frequency comb around 4 μm, and present an experimental comparison of the performance of half-harmonic generation using PPLN [11], OP-GaAs and OP-GaP. Despite the higher nonlinearity of GaAs and its comparable group delay dispersion to GaP, GaP-based half-harmonic generation has a significantly better performance. We achieved ~220 mW of average power at 250 MHz corresponding to ~43% of conversion efficiency. The OP-GaP-based half-harmonic OPO is pumped by the output of another half-harmonic OPO operating at 2.1 μm. The resulting frequency combs are intrinsically phase- and frequency-locked to the output comb of the mode-locked Yb:fiber laser driving the cascaded half-harmonic generation processes [11].

2. Materials for quasi-phase matched half-harmonic generation at 4 μm

Efficient half-harmonic generation of short-pulse frequency combs around 4 μm is important because it can lead to intrinsically frequency-locked frequency combs in an important molecular spectroscopic window using well-developed frequency comb sources at 2 or 1 μm [11]. Moreover, one can use the resulting mid-IR frequency comb to pump another stage of half-harmonic generation and access the long-wavelength mid-IR window. To demonstrate the advantages of using OP-GaP for half-harmonic generation of few-cycle pulses around 4 μm, we have compared its properties with other available materials, suitable for quasi-phase matched operation around 4.2 μm, i.e. PPLN and OP-GaAs. The relevant parameters of the crystals are summarized in Table 1.

PPLN demonstrates the lowest nonlinear coefficient. However, because of its technological maturity, one can use long large-aperture samples of excellent optical quality. At the same time, 4.2 μm is approaching the edge of the PPLN transparency region, which results in a large GVD to be compensated, and even a larger TOD at the central wavelength. Also, we expect the long-wavelength wing of the generated spectrum to be cut below 5 μm due to the fundamental absorption. OP-GaAs and OP-GaP possess none of these drawbacks, and from the numbers presented in Table 1 we might assume OP-GaAs should demonstrate a

Optics EXPRESS

significantly lower threshold than OP-GaP in equal conditions. One may be able to partially compensate that by using a longer OP-GaP crystal due to its lower group velocity mismatch. In the experimental results presented here, we compare the performance of half-harmonic generation for these three materials at around 4.2 μm.

Table 1. Optical parameters of $LiNbO_3$, GaAs and GaP

	PPLN	Op-GaAs	Op-GaP
Nonlinear coefficient	d_{33} = 18.7 pm / V [24]	d_{14} = 94 pm / V pm/V [24]	d_{14} = 28 pm / V [25,26]
Index of refraction	n = 2.05	n = 3.30	n = 3.01
F.O.M. (d_{eff}^2 / n^3)	41	326	38
Group velocity dispersion (GVD)	–1861 fs^2/mm	+ 372 fs^2/mm	+ 114 fs^2/mm
Third order dispersion (TOD)	+ 16200 fs^3/mm	+ 1471 fs^3/mm	+ 1545 fs^3/mm
Period for 4.2 μm OPO	32 μm	63.5 μm	93 μm
2.1–4.2 μm group velocity mismatch	–241 fs/mm	298 fs/mm	150 fs/mm
Optimal length for 50-fs pulse	0.42 mm	0.34 mm	0.67 mm
Transparency region	0.4–5 μm	0.85–18 μm	0.57–12 μm

All data correspond to ~4.2 μm wavelength. The effective nonlinear coefficient is $d_{eff} = d_{33}$ for PPLN and $d_{eff} = 1.155 d_{14}$ for GaP and GaAs according to crystal orientations [24]. The nonlinear coefficient for GaP is wavelength-corrected using the Miller's rule [27]. The optimal length has been estimated assuming that the OPO and pump pulse durations are close, and that the group delay mismatch should not exceed their sum. Figure of merit (F.O.M) is often used for estimating the parametric gain in c.w. or quasi-c.w. OPOs [28]. GVD and TOD are the second and third derivatives of the wavenumber in the medium with respect to angular frequency, respectively.

3. Experimental setup

The cascaded half-harmonic OPOs are synchronously pumped [Fig. 1] by a 1-W mode-locked Yb:fiber laser at 1 μm, with ~70-fs pulses and a repetition rate of 250 MHz. The first OPO is a PPLN-based half-harmonic OPO converting the pump to ~500 mW of ~50-fs pulses at 2.09 μm [11].

Similar to [11], the second OPO is pumped by the signal output of the first OPO. Two concave gold mirrors (M6 and M7) have ROC of 25 mm. This results in the waist diameter of 27 μm in the middle of the stability range. The distance between mirrors between M4 and M5 is chosen to image the secondary beam waist of the 2-μm OPO onto the secondary beam waist of the 4-μm OPO. The 2-μm beam is thus focused to the same confocal parameter of 0.26 mm, but has a 20-μm waist diameter. The exact mode matching is traded off in favor of the Gouy-phase matching, making sure that the setup accommodates samples of any thickness. Passing through the substrates of M4 and M5 mirrors substrate results in a certain negative chirp of the pump pulse. We estimate the pump pulse duration of about 55 fs at the crystal entrance, which is nearly two times longer than the transform-limited pulse width of 29 fs, corresponding to the 170-nm broad spectrum at 2.09 μm. The input pulse duration can be reduced close to the transform-limited value by pre-compensation, but this was not necessary, as the threshold was low enough for all tested samples.

Optics EXPRESS

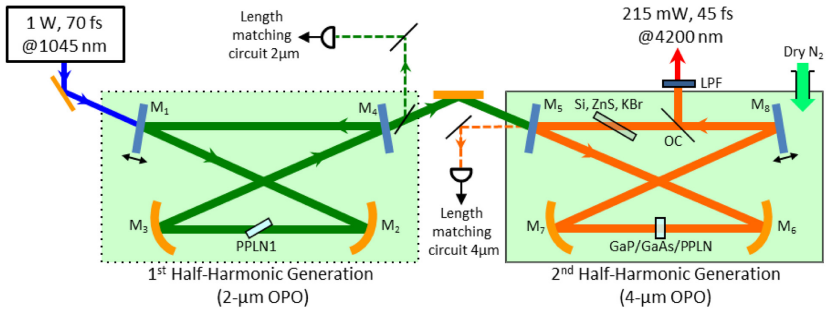

Fig. 1. Schematic of the experiment comprising two half-harmonic OPOs. OC, pellicle-type output coupler. Si, ZnS and KBr denote Brewster-angled dispersion compensating elements.

The nonlinear gain is provided by a plane-parallel OP-GaP crystal with a poling period of 92.7 μm for type-0 phase matching at room temperature, which has broadband anti-reflection (AR) coating for the wavelength region around 4.2 μm with another reflection minimum at pump wavelength of 2.09 μm. To make fair comparison, we have tested samples with 1, 0.5, and 0.25 mm thickness, as well as a 0.25-mm thick OP-GaAs in the same orientation and a 1-mm thick PPLN crystal, both AR coated for pump and degenerate OPO wavelength regions. For dispersion compensation, we used plan-parallel plates of different optical materials placed in the cavity at Brewster angle: ZnS and KBr for OP-GaP and OP-GaAs and Si for PPLN. This allowed compensating the round-trip group delay dispersion (GDD) of the nonlinear crystal below 100 fs^2 for all samples, but the TOD remained uncompensated [Fig. 2]. It must be noted here that all dielectric coatings contributed additional dispersion. From the data provided by the vendors, each dichroic mirror bounce added ~22 fs^2 of GDD and ~3750 fs^3 of TOD at 4200 nm. The antireflection coatings on OP-GaAs and OP-GaP contributed negligible GDD and only ~140 fs^3 of TOD per pass at the same wavelength.

The output coupling of the mid-IR signal pulses for the OP-GaAs and OP-GaP OPOs is provided by one or two coated pellicles, providing ~15-30% of reflection each, depending on the incidence angle. At 45°, the pellicle reflectivity is about ~25% at 4.2 μm. For the results presented here, we did initial adjustments to the configurations of the output couplers to achieve the highest output power at the highest available pump power. For the PPLN OPO, optimum output coupling is achieved with angle tuning of a Si slab [11].

The 4-μm OPO resides in a box purged with dry nitrogen to reduce the effects of atmospheric absorption on the OPO operation. The effect of nitrogen purging was to decrease the threshold and improve the efficiency of OPO operation by about 1.4 times, and to broaden the range of cavity lengths, at which OPO was still operating. The threshold of the 4-μm OPO is

Optics EXPRESS

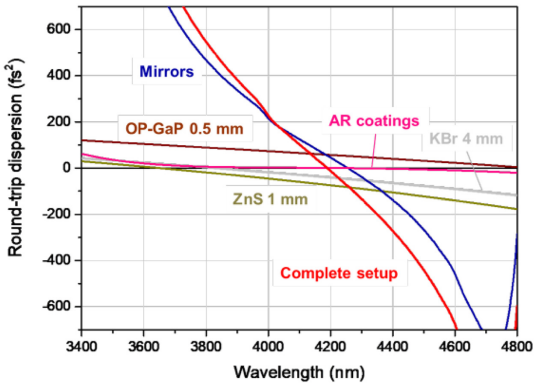

Fig. 2. Intracavity round-trip dispersion.

200-300 mW with ~25% output coupling and 26 mW without output coupling. The lengths of both OPOs have been locked using the dither-and-lock procedure described in Ref [10].

4. Results and discussions

We first preset the results of half-harmonic generation using OP-GaP. Without output coupling, the OPO using a 1 or 0.5-mm OP-GaP sample exhibits a threshold of a few tens of milliwatts even without nitrogen purging, but with quite low output power. After initial adjustment, we tuned the output coupling from ~25% to ~44% (by angle tuning one or two pellicles). With compensated dispersion, the maximum output power at the open air would typically be 150-175 mW, increasing to 190-220 mW after few minutes of nitrogen purging. The results of the OPO with 1-mm and 0.5-mm OP-GaP are quite comparable (Table 2), with a slightly better performance by the 0.5-mm sample, which has been chosen for the detailed study.

The dispersion of a 0.5-mm GaP crystal (57 fs^2) and the two reflections from the dichroic mirrors (~43 fs^2) is compensated by a 1 mm-thick ZnS plate at Brewster angle (–75 fs^2), resulting in about ~25 fs^2 of uncompensated GDD, which is additionally reduced to ~-15 fs^2 by inserting a 4-mm KBr plate at Brewster angle (~-40 fs^2). At 500 mW of pump power, the OPO emitted 215 mW of output from a single ~25% output-coupling pellicle. The output spectrum is shown in Fig. 3(a). It is centered at 4.18 μm with the 3-dB bandwidth of ~690 nm, and the –30 dB width of ~2 μm. The double-peaked cut in the spectrum around 4.2 μm corresponds to the CO_2 absorption in the 1.5 m beam path from the OPO to the spectrometer.

Optics EXPRESS

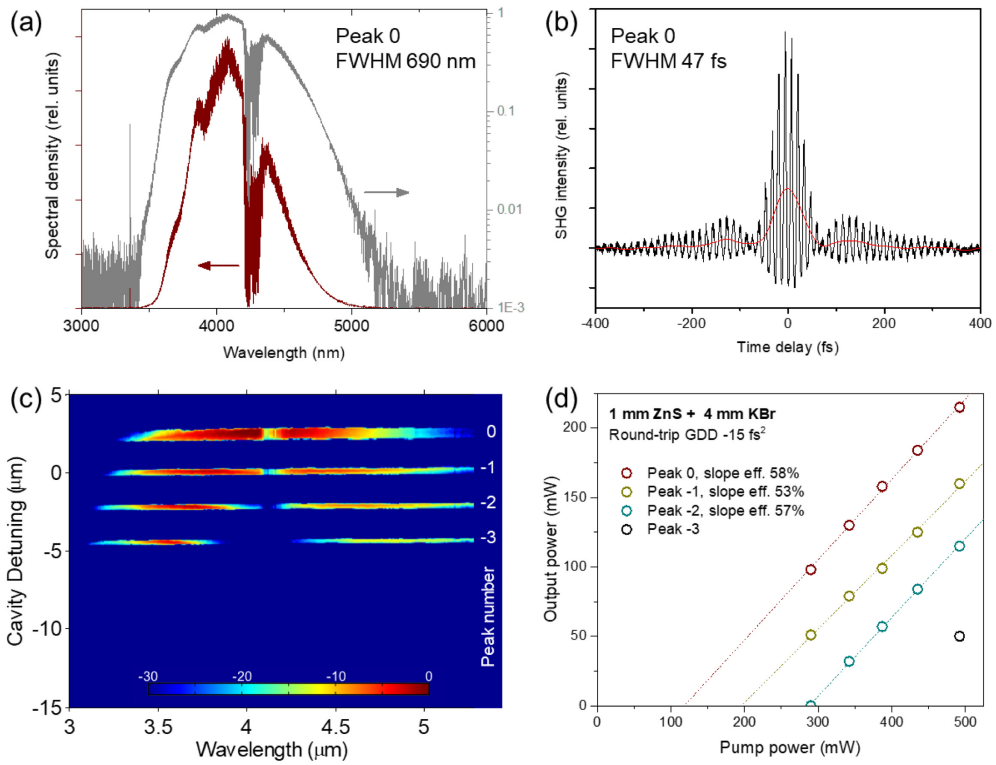

Fig. 3. Optical spectrum in linear and log scale (a), autocorrelation trace (b, black: interferometric, red: intensity), output spectrum as a function of cavity length (c), and output power (d) of the of the 0.5-mm OP-GaP OPO.

The autocorrelation of the pulses is measured by a two-photon extended-InGaAs detector and is shown in Fig. 3(b). The pronounced autocorrelation wings are due to the dispersion associated with the CO_2 absorption in the beam path outside of the resonator. From this autocorrelation, one can estimate ~47 fs of pulse duration. Taking the same spectrum without the CO_2 absorption produces a transform-limited spectrum of ~38-fs pulse duration. A scan of the cavity length and measuring the input-output dependencies [Fig. 3(d)] allows identifying the highest-power peak, which corresponds to nearly exact length match, i.e. synchronous propagation of the pump and the OPO pulse [Fig. 3(c)]. The peaks −1, −2, and −3 correspond to the case when the OPO cavity round-trip is shorter than the pump repetition period by one, two, and three half-periods, respectively (negative detuning). These peaks demonstrate increasingly higher threshold, and nearly the same slope efficiency [Fig. 3(d)], but become non-degenerate with increasing detuning. It is interesting to note that the spectrum and temporal shapes of the output pulses for peaks 0 and −1 do not change over the range of the pump powers used in Fig. 3(d), meaning that the spectrum width is governed by the intracavity dispersion and losses rather than nonlinear effects.

The described configuration corresponded to a slight dispersion overcompensation. Figure 4 demonstrates the performance of the OPO with undercompensation [Figs. 4(a) and 4(b)] and stronger overcompensation [Figs. 4(c) and 4(d)]. One can observe a slightly higher threshold, but quite comparable slope and overall efficiency, as well as the spectral width, being 650 nm for overcompensated and 720 nm for the undercompensated configurations. It is interesting to note that degenerate operation occurs not only for the nearly synchronous “0” peak, but also for a long-cavity peak where the intracavity signal pulse receives a group delay by a half-period relative to the pump pulse on each round-trip (peak “1”). This peak exhibits a high oscillation threshold and a large slope efficiency, both of which are signs of formation of

Optics EXPRESS

simultons [29]. Simulton formation in the mid-IR can lead to even shorter pulses and higher conversion efficiencies, which will be the subject of future work.

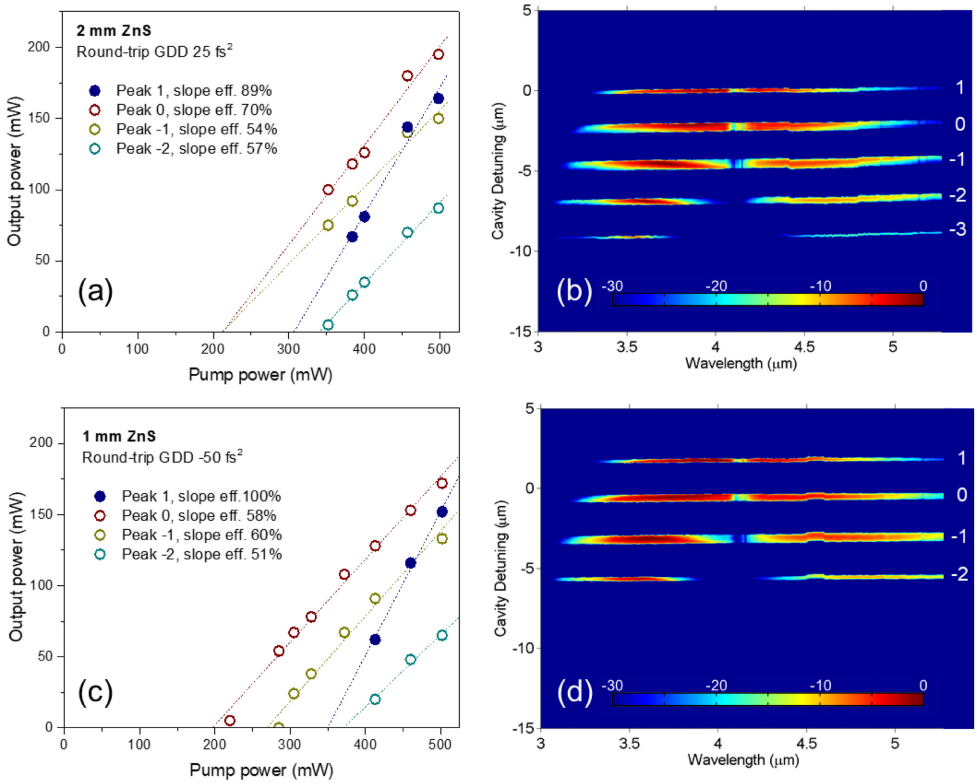

Fig. 4. Output power (a,c) and output spectrum as a function of cavity length (b,d) of the of the 0.5-mm OP-GaP OPO with different round-trip dispersions.

In Table 2 we summarize the results obtained with OP-GaP samples of different thickness as well as PPLN and OP-GaAs. PPLN has a large dispersion and material absorption, which limit the spectral bandwidth to about 260 nm with pulse durations longer than 100 fs. It also leads to a higher threshold and a lower slope efficiency compared to an OP-GaP sample of similar length. OP-GaAs demonstrates a large bandwidth and short pulses, set by the bandwidth limitations of the setup mostly arising from the uncompensated higher-order dispersions. However, the OP-GaAs sample demonstrates the same threshold and a lower conversion efficiency even compared to the 0.25-mm OP-GaP sample, while it was expected to outperform the 0.5-mm OP-GaP, which had a similar dispersion, but much lower F.O.M. This behavior – broad bandwidth, but fairly low conversion efficiency is consistent with previous OP-GaAs experiments with Tm-fiber and Cr:ZnS laser pumping [15, 17, 18, 30]. Understanding the underlying physics of such a behavior requires a more comprehensive study and will be the subject of future research, however, we point out a few potential reasons here. One possibility is the residual absorption of the OP-GaAs material in the 4-μm region [30]. To make such a clear distinction in OPO performance, however, the absorption in the GaAs must far exceed the absorption in GaP at 4 μm and approach ~10%; also the difference in absorption does not explain the comparable threshold values despite the large F.O.M. difference. We therefore believe that the lower-power operation of the OP-GaAs OPO is most likely due to one or a combination of nonlinear effects, for instance the three-photon absorption of the pump, two-photon absorption at the sum-frequency of pump and signal at

Optics EXPRESS

around 1.4 μm, Kerr lensing, and/or nonlinear dynamics [29]. Three-photon absorption in GaAs has been shown to limit the OPO performance up to 2.5 μm [31].

Table 2. Summary of the experimental results.

	PPLN	GaP			GaAs
Sample thickness	1 mm	1 mm	0.5 mm	0.25 mm	0.25 mm
GDD compensation	5 mm Si	2 mm ZnS	1 mm ZnS + 4 mm KBr	4 mm KBr	1 mm ZnS
Material GDD	40 fs^2	–40 fs^2	–20 fs^2	–10 fs^2	–20 fs^2
Material TOD	20600 fs^3	4400 fs^3	2200 fs^3	1170 fs^3	2200 fs^3
Round-trip GDD	85 fs^2	5 fs^2	–15 fs^2	35 fs^2	25 fs^2
Round-trip TOD	28400 fs^3	12200 fs^3	10000 fs^3	9000 fs^3	10000 fs^3
Threshold	~1 nJ (250 mW)	~0.4 nJ (100 mW)	~0.5 nJ (125 mW)	~1 nJ (250 mW)	~1 nJ (250 mW)
Slope efficiency	30%	50%	59%	40%	25%
Range of output coupling tuning	~20%	~25-45%	~25-45%	~20%	~20%
Max. output power	75 mW	200 mW	215 mW	100 mW	60 mW
Spectrum FWHM	265 nm	500 nm	690 nm	695 nm	630 nm
Min. duration FWHM	110 fs	60 fs	45 fs	45 fs	50 fs

The dispersion data corresponds to 4.2 μm.

5. Conclusion

We reported a two-stage cascaded half-harmonic generation of three-optical-cycle pulses (<50 fs) centered around 4.2 μm corresponding to a broadband mid-IR frequency comb. The second stage of half-harmonic generation is achieved using OP-GaP, and the resulting frequency comb is intrinsically phase- and frequency-locked to the mode-locked fiber laser pump at 1 μm. In contrast to previous demonstrations, the mid-IR OP-GaP-based half-harmonic generation is characterized by a high conversion efficiency of ~43%, and an output power of 220 mW, with nearly 1 nJ pulse energy, and few-cycle pulses.

We experimentally verify that using OP-GaP in this spectral range is preferable over OP-GaAs, and we expect to extend this work to simulton-based half-harmonic generation [29], which can potentially lead to higher efficiencies and shorter pulses. Further simplification of the setup can be reached by replacing the first stage of half-harmonic generation with a fiber laser source. Using the Tm-fiber laser, Raman-shifted to 2.1 μm [32], we have been able to operate the OP-GaP OPO with only 2 nJ of threshold energy at 150 fs pulse duration and up to 40 mW of output power at 80 MHz repetition rate.

Funding

NFR Nano 2021 (N219686); FWF (P24916); NSF (ECCS-1609688); NSF-BSF (PHY-1535711).

Acknowledgments

The authors would like to thank M. Jankowski for discussions, and C. Langrock and K. A. Ingold for experimental support.